Title

Cellular Assays for Studying the Fe–S Cluster Containing Base Excision Repair Glycosylase MUTYH and Homologs

Authors

Majumdar, Chandrima
Nuñez, Nicole N
Raetz, Alan G
et al.

Publication Date

2018

DOI

10.1016/bs.mie.2017.12.006

Peer reviewed

HHS Public Access

Author manuscript

Methods Enzymol. Author manuscript; available in PMC 2019 January 10.

Published in final edited form as:

Methods Enzymol. 2018 ; 599: 69–99. doi:10.1016/bs.mie.2017.12.006.

Cellular assays for studying the Fe-S cluster containing base excision repair glycosylase MUTYH and homologs

C. Majumdar[*], **N.N. Nuñez**[*], **A.G. Raetz**[*], **C. Khuu**[*], and **S. S. David**[*,1]

* University of California, Davis, at Davis, CA, United States

Abstract

Many DNA repair enzymes, including the human adenine glycosylase MUTYH, require iron-sulfur (Fe-S) cluster cofactors for DNA damage recognition and subsequent repair. MUTYH prokaryotic and eukaryotic homologs are a family of adenine (A) glycosylases that cleave A when mispaired with the oxidatively damaged guanine lesion, 8-oxo-7,8-dihydroguanine (OG). Faulty OG:A repair has been linked to the inheritance of missense mutations in the *MUTYH* gene. These inherited mutations can result in the onset of a familial colorectal cancer disorder known as MUTYH-associated polyposis (MAP). While *in vitro* studies can be exceptional at unraveling how MutY interacts with its OG:A substrate, cell-based assays are needed to provide a cellular context to these studies. In addition, strategic comparison of *in vitro* and *in vivo* studies can provide exquisite insight into the search, selection, excision process, and the coordination with protein partners, required to mediate full-repair of the lesion. A commonly used assay is the rifampicin resistance assay that provides an indirect evaluation of the intrinsic mutation rate in *Escherichia coli* (*E. coli* or *Ec*), read out as antibiotic resistant cell growth. Our laboratory has also developed a bacterial plasmid- based assay that allows for direct evaluation of repair of a defined OG:A mispair and provides important information on the impact of functional defects that alter affinity and excision on overall repair. Finally, a mammalian GFP-based reporter assay more accurately models features of mammalian cells and therefore provides useful information on the cellular repair properties of MUTYH. Taken together, these assays help to provide cellular context to the interaction of MUTYH and its homologs in how they are able to prevent the accumulation of G:C to T:A transversion mutations and a disease phenotype.

Keywords

MutY; MUTYH; Base excision repair; glycosylase; Fe-S clusters; GFP reporter assay; 8-oxoguanine; rifampicin resistance; bacterial repair assays

1. Introduction

Bacterial MutY and its mammalian MUTYH homologs are glycosylases that catalyze the excision of adenine mispaired opposite 8-oxo-7,8-dihydroguanine (OG) as the first step in base excision repair (BER) to prevent OG-mediated G:C→T:A transversion mutations (David, et al., 2007). These glycosylases carry a $[4Fe\text{-}4S]^{2+}$ (Fe-S) cluster coordinated by

[1]Corresponding author: ssdavid@ucdavis.edu.

four Cys residues, two of which anchor a solvent exposed Fe-S cluster loop (FCL) containing positively charged amino acid residues that have been implicated in DNA binding and enabling subsequent catalysis (Chepanoske, et al., 2000). Compromised activity of inherited variants of MUTYH has been linked to a familial colorectal cancer (CRC) syndrome called MUTYH-associated polyposis (MAP) (Al-Tassan, et al., 2002). Individuals with MAP exhibit colorectal polyposis and have a high likelihood of eventual colorectal cancer onset (Jenkins, et al., 2006;Farrington, et al., 2005) due to an accumulation of G:C to T:A transversion mutations in the *adenomatous polyposis coli (APC)* tumor suppressor gene (Al-Tassan, et al., 2002;Sieber, et al., 2003) (Viel, et al., 2017).

The discovery of MAP spurred interest in understanding how specific MAP variants alter the protein structure and associated enzymatic activity of MUTYH. Interestingly, many MAP variants are located in regions near the Fe-S cluster (Figure 1) and have the potential to disrupt metal coordination and proper positioning of the FCL residues for mismatch engagement (Banda, et al., 2017). In our laboratory, the functional properties of the first identified MAP variants (Tyr165Cys and Gly382Asp in human MUTYH) were assessed using kinetic and binding assays. These experiments were initially performed using the corresponding variants in *Escherichia coli (E. coli* or *Ec)* MutY (Tyr82Cys and Gly253Asp) (Al-Tassan, et al., 2002) and revealed a compromised adenine glycosylase activity on G:A and OG:A mispair-containing substrates. Our laboratory also showed that both variants have a compromised affinity for an OG:FA-containing substrate analog duplex (where FA = 2'-fluoroadenosine) relative to that of the WT enzyme (Chmiel, et al., 2003) Subsequent analysis of the corresponding variants in the mouse homolog Mutyh (expressed in bacteria) and the insect-cell expressed human MBP-MUTYH protein indicated similarly reduced levels of activity (Engstrom, et al., 2014;Pope and David, 2005;Brinkmeyer and David, 2015;Kundu, et al., 2009). *In vitro* kinetics and binding studies of *Ec* MutY has also been useful in establishing the importance of the Fe-S cluster domain in substrate recognition and excision by MutY(Chepanoske, et al., 2000). An accompanying MutY chapter in this volume provides additional details regarding *in vitro* experiments.

In vitro analyses were a key element in cementing the link between inheritance of catalytically compromised MUTYH variants and colorectal cancer (Al-Tassan, et al., 2002;David, et al., 2007). A notable feature of the *in vitro* studies of Tyr165Cys and Gly382Asp, as well as the corresponding mutated versions in the bacterial and murine enzymes, was that the adenine excision activity of the Tyr-to-Cys variants was consistently more compromised than that of the Gly-to-Asp variants. This difference could be interpreted as implicating a higher CRC predisposition for individuals with Tyr165Cys over Gly382Asp; however, we also considered that the activity of Gly382Asp MUTYH may be more compromised in a cellular context. Indeed, *in vitro* experiments are limited in accurately mimicking the activity of MUTYH in a cellular environment. For example, within mammalian cells, MUTYH is subject to transcriptional regulation (Fry, et al., 2008) and undergoes post-translational protein modifications such as phosphorylation and ubiquitination (Kundu, et al., 2010;Dorn, et al., 2014). Furthermore, cellular DNA is packaged within chromatin structure and access to genomic DNA for repair is regulated by epigenetic factors (Amouroux, et al., 2010) (Menoni, et al., 2017).

The cellular environment also requires that MUTYH searches for OG:A mispairs within the vast excess of undamaged genomic DNA; this complicating feature is clearly not accounted for in *in vitro* assays, which use short 30 base pair (bp) duplexes. Moreover, the search process inside cells is likely highly coordinated with other processes in the cell, such as replication and transcription, and requires precise interactions with other protein partners. Several MUTYH-protein interactions have been identified such as interactions with the downstream AP site processor protein, AP endonuclease 1, and the Proliferating Cellular Nuclear Antigen (PCNA) sliding DNA clamp (Parker, et al., 2001). In addition, MUTYH also interacts with proteins from other DNA repair pathways outside of BER, such as the mismatch repair protein MSH6a (Gu, et al., 2002) and the epigenetic regulator SIRT6 (Hwang, et al., 2015). Intriguingly, MUTYH also interacts with the Hus1 protein of the Rad9-Rad1-Hus1 (911) DNA damage sensing complex, suggesting a role in mediating signaling cascades during the response to oxidative stress (Turco, et al., 2013;Shi, et al., 2006).

Structural and functional studies have elucidated features of MutY and its substrates that are important for recognition and catalysis (Banda, et al., 2017;Manlove, et al., 2016). However, the relative importance of specific features of mismatch repair and adenine excision in overall cellular repair remains unclear. To address these issues, we have developed bacterial cell assays to evaluate the impact of specific modifications of the OG or A in the OG:A substrate (Manlove, et al., 2017;Livingston, et al., 2008), or to evaluate specific amino acid variations in MutY, on the overall repair in cells (Brinkmeyer, et al., 2012). These studies have revealed that features that aid in recognition of OG within the OG:A mispair are the most important for mediating high levels of overall repair. Indeed, we have found that "binding" defects measured *in vitro* are magnified in a cellular context, consistent with the stringent requirements for base pair location and discrimination. For example, we recently showed using a battery of OG analogs that initial recognition of an OG:A mispair and discrimination from a T:A bp may be attributed to a single interaction with the 2-amino group of OG localized in the major groove (Manlove, et al., 2017). These studies with substrate analogs illustrate the power of such cellular assays to reveal unique molecular details that are most impactful to cellular repair.

Using cell-based assays, it will be possible to more fully evaluate the roles of the MutY/MUTYH Fe-S cluster. In addition, these assays will allow researchers to consider the implications of Fe-S cluster associated variants in the development of MAP. In some cases, analysis of variations in the MUTYH protein *in vitro* may be difficult due to challenges with expressing and purifying mammalian homologs. This obstacle is also further highlighted by the observation that mutations to residues surrounding the Fe-S cluster can result in disruption of protein folding and consequently poor protein yields (Chepanoske, et al., 1999;Golinelli, et al., 1999). As a result of these limitations, the development of cellular assays is crucial for understanding MUTYH function on many levels and will be especially useful for understanding the consequences of mutations to the Fe-S cluster coordinating ligands and surrounding amino acids, and delineating the effects of adjacent MAP variants (Brinkmeyer, et al., 2012;Golinelli, et al., 1999;Raetz, et al., 2012).

In this chapter, we describe the cellular assays that have been developed in our laboratory to probe the features of MUTYH mediated repair. We elaborate on studies using rifampicin reversion assays to indirectly monitor deficiencies in MUTYH activity by measuring the mutation frequency of cells expressing a MUTYH variant. In addition, we detail the protocols of bacterial and mammalian cell assays that employ a reporter plasmid to quantify substrate specific repair by MutY/MUTYH variants. These techniques in combination with *in vitro* characterization of MutY enzymes, described in the accompanying chapter, make it possible to holistically understand the role(s) of the Fe-S cluster within MutY/MUTYH, and the intimately related roles of MUTYH in diseases, such as MAP.

2. Mutation suppression activity measured in Rifampicin Resistance Assays

2.1. Overview of the Rifampicin Resistance Assay

The *MutY* gene was initially discovered as a locus that resulted in increased G:C to T:A transversion mutations when disrupted (David, et al., 2007;Miller and Michaels, 1996;David and Wiliams, 1998) A convenient method for analyzing mutation frequency in *Ec* uses the ability of the antibiotic rifampicin to block bacterial RNA polymerases (Wehrli, et al., 1968). *Ec* strains lacking *mutY* and *mutM* (MutM removes OG from OG:C bps), exhibit extremely high levels of G:C to T:A mutations in the *rpoβ* gene that results in modification of the rifampicin binding pocket and consequently, an increase in the frequency of surviving colonies on rifampicin selection plates (Figure 2) (Garibyan, et al., 2003). The mutation frequency is reduced, as inferred from reduced number of colonies in the presence of rifampicin, by expression of MutY or MUTYH on a plasmid- vector. The supplemented gene is able to complement for the lack of the bacterial MutY, providing a useful means to analyze the activity of a MutY or MUTYH variant in these bacterial cell assays (Chmiel, et al., 2003;Golinelli, et al., 1999;Slupska, et al., 1999)

Site-directed mutagenesis of individual *Ec* MutY Fe-S cluster Cys ligands to Ser, His, and Ala followed by evaluation in the rifampicin resistance assays demonstrated varying abilities to suppress mutation frequency depending on the Cys ligand replaced (Golinelli, et al., 1999). For example, expression of *Ec* MutY where the Fe-S cluster ligand, Cys199 was replaced with Ala, Ser or His resulted in similar low numbers of rifampicin resistant (Rif^R) colonies as WT, suggesting flexibility in amino acid replacements at position 199 of MutY. Notably, in the case of Cys199Ala, the polypeptide chain could not be detected in overexpression tests, suggesting that loss of this Fe-coordinating ligand makes the enzyme exceedingly unstable. This result indicates that within these cellular assays, very low levels of active protein are needed to study the effects of the mutants. A distinctly different trend was observed at position 192, where relative levels of overexpression (Cys192His > Cys192Ser > Cys192Ala) were found to not correlate with relative ability to suppress mutations (Cys192Ser > Cys192Ala > Cys192His) (Golinelli, et al., 1999). In this case, modification at Cys192 not only affects stability, but also the ability to properly mediate repair of OG:A mismatches and prevent mutations.

2.2. Transformation and Growth of Cells

This rifampicin resistance assay follows closely to a previously published protocol for analyzing mutated versions of MutY with the following added specifications for analyzing MUTYH (Golinelli, et al., 1999). The *Ec* strain used in the rifampicin resistance assay is the GT100 y^-m^- cell line that lacks functional MutY and OG glycosylase MutM. Previous work has shown that only in the absence of both glycosylases are the levels of G:C to T:A transversions high, consistent with both enzymes acting on OG lesion substrates to prevent mutations (Michaels, et al., 1992). Transformation of a *pMAL-c2x* expression plasmid bearing the WT *MBP-MUTYH* gene into the GT100 y^-m^- cells significantly reduces the number of rifampicin revertant colonies, resulting in a lower mutation frequency compared to GT100 y^-m^- cells alone and GT100 y^-m^- cells carrying the *pMAL-c2x* empty vector (Kundu, et al., 2009).

The *pMAL-c2x* (NEB) expression plasmid containing the WT *MBP-MUTYH* gene, for example, is transformed via heat shock into chemically competent *Ec* GT100 y^-m^- and plated onto LB agar plates (Table 1) and incubated overnight at 37 °C (Table 3). Each trial is comprised of n=15 for WT as well as for each associated variant being tested to account for the variability in mutation onset during cell growth. Single colonies are selected to inoculate liquid cultures (1 ml each, Table 1) and allowed to grow for 16-18 h at 37 °C and 220 rpm (Table 3). Colonies are picked based on morphology and isolation to ensure the analysis of the mutation rate of a single starter *Ec* colony. An assumption made when selecting colonies is that a single colony likely represents over 10^7 cells (Lodish, et al., 2000), and that these colonies are progeny of a mutant conferring rifampicin resistance.

2.3. Determining the Mutation Frequency

The following day, culture agar and rifampicin agar are warmed at 37 °C for 1 h prior to plating. 100 μl of a 10^{-7} dilution is plated on culture agar plates to determine the number of viable cells, while 100 μl of the undiluted culture is plated onto the rifampicin selection plates (Table 1) to determine the number of resistant colonies. The plates are incubated at 37 °C for 16 h, after which the number of colonies on each plate is counted. The mutation frequency (f, x 10^{-8}) is calculated below by equation (1) for each trial:

$$f = \frac{\text{median number of resistant colonies}}{\text{average number of viable colonies}} \quad 1$$

It is important to note that the mutation frequency is the proportion of cells in a population that are mutated, but this cannot be directly equated with the population's mutation rate (Foster, 2006) (Rosche and Foster, 2000). The majority of colonies likely arises from cells that developed a mutation during the incubation process and consequently, these cells and their progeny will confer rifampicin resistance. Thus, a single mutation early in the growth period yields an exponential number of mutant colonies as its progeny (Rosche and Foster, 2000). A particular culture may have had a low mutation rate, but due to random chance, it can generate assay results with high mutant counts. As a result, the relationship between cellular mutation rate and number of mutants at the endpoint is a complex function.

Fortunately, continual improvement to mathematical models have recently converged on a set of guidelines that are both statistically rigorous and easily accessible to experimentalists (Zheng, 2015). Notably, the Ma-Sandri-Sarkar (MSS) maximum likelihood estimator (Sarkar, et al., 1992) has been shown to be a robust estimator of mutation rate (Couce and Blazquez, 2011). Recent web-based bioinformatic programs simplify maximum likelihood analysis (Gillet-Markowska, et al.,2015). In the following section, we will discuss an application of one such method to compare the mutation rate of WT and a mutant MUTYH.

2.4. Case Study: Use of Rifampicin resistance assay to characterize Zn- linchpin motif in MUTYH

In addition to the Fe-S cluster, the mammalian homologs, Mutyh and MUTYH, have been found to possess a Zn^{2+} ion within the interdomain connecter (IDC) that connects the catalytic N-terminal and OG-recognition C-terminal domains. The critical importance of the Zn^{2+} ion within the IDC, resulting in its designation as the “Zinc- linchpin” motif, was determined using metal analysis and *in vitro* activity assays of Cys to Ser mutations in the mouse Mutyh homolog, along with rifampicin resistance assays of the analogous versions of MUTYH (Engstrom, et al., 2014). Replacement of two Cys ligands (Cys325/307 and Cys328/310 in human/mouse enzyme) with Ser resulted in reduced levels of Zn^{2+} and Fe-S cluster (Engstrom, et al., 2014) Evaluation of these same mutations in human MUTYH showed a substantial increase in mutation frequency compared to WT when evaluated using the rifampicin resistance assay (Engstrom, et al., 2014).

In Table 2, we have shown representative data for one trial of the rifampicin resistance assay for the Cys325Ser MUTYH relative to WT MUTYH. In this experiment, each trial is comprised of at least fifteen individual cultures of the same genotype. Each data set is entered into the *bzRates* calculator (http://www.lcqb.upmc.fr/bzrates) to get a mutation rate per cell division shown in the last two rows of Table 2, with additional correction for the 10^7 dilution factor. In our case, relative fitness of the mutants to wild type is not known and 100 μl of 1 ml culture was used for plating efficiency. Our laboratory and others (Wolff, et al., 2004) have reported the median number of rifampicin revertant colonies divided by the average number of cells in an untreated control as the mutation frequency (Engstrom, et al., 2014;Kundu, et al., 2009;Brinkmeyer, et al., 2012;Golinelli, et al., 1999;Chmiel, et al., 2003). When the Cys325Ser MUTYH variant was transformed into GT100 y^-m^- cells, the mutation frequency of cells containing this variant was greater than 11 fold higher than WT (Engstrom, et al., 2014), consistent with the analysis in Table 2.

Troubleshooting tips: Due to the large variability in cellular assays, it is imperative to ensure a proper sample size when using the rifampicin resistance assay. As evidenced in Table 2, the number of colonies spans a wide range, and therefore, each trial should contain a minimum of 15 colonies due to the variability in cell growth, as fewer cultures can result in a misrepresentation of the mutation frequency of the enzyme. Furthermore, we recommend running a wild-type enzyme (or other control) alongside every set of mutants for proper comparison of colonies. In the case of consistently high numbers of mutant colonies, especially in the wild type, rifampicin selection plates should be poured again and used within a week to ensure efficacy of the antibiotic. Plates should be dark red in color while

being used, as they become lighter as they lose the ability to disrupt RNA polymerase function.

3. Analysis of MutY-mediated repair of defined plasmid substrates in *E. coli*

3.1. Designing a Plasmid Based Bacterial Cell Assay

In the accompanying chapter in this volume, we have described various *in vitro* assays utilized by our laboratory (Brinkmeyer and David, 2015;Chepanoske, et al., 1999;Porello, et al., 1998) to measure kinetic parameters of MutY enzymes. These assays typically use a substrate mispair within a defined 30 bp duplex. These *in vitro* assays allow for quantitative determination of substrate binding affinities and rates of the base excision reaction. However, the relationship of the enzymatic parameters to overall repair in a more complex biological context is important to delineate. Indeed, the task required of MutY in cells to recognize a single OG:A mispair amongst the large excess of similar bps would be expected to be more challenging than within a short DNA duplex. To address these issues, we have developed a plasmid-based assay that allows for evaluating MutY (WT or variant) mediated repair of a defined substrate within plasmid DNA in bacteria. By comparing *in vitro* enzymatic and binding parameters to the extent of repair in the plasmid-based cellular assays, we have revealed distinct structural features of the OG:A mispair and MutY that are important for various steps in the detection, engagement and excision process of BER (Manlove, et al., 2017) (Brinkmeyer, et al., 2012;Livingston, et al., 2008). The important features of the OG:A substrate have been revealed by evaluating the MutY-mediated repair of synthetically derived modified substrates, such as OI:A (where OI = 8-oxoinosine) (Manlove, et al., 2017;Livingston, et al., 2008). We have also evaluated the repair of variants of catalytic residues in *Ec* MutY (such as Asp138Cys MutY) on OG:A repair (Brinkmeyer, et al., 2012). Ongoing efforts in our laboratory are aimed at using these assays to perform similar studies to address the roles of the Fe-S cluster and the FCL motif in MutY.

This assay measures the cellular repair activity of MutY in terms conversion of a strategically placed OG:A lesion to G:C in *Ec* cells; full repair requires the initial MutY initiated removal of A, and then subsequent BER, and action of MutM to provide the G:C bp (Figure 3). The key feature of this assay is placement of the OG:A bp at a potential Bmtl restriction site such that MutY-mediated repair leads to creation of a restriction site that can be monitored by restriction digestion. Lack of MutY-mediated repair of OG:A leads to significant levels of T:A at the lesion site. The %G:C bps in cells possessing MutY is compared to those lacking MutY to determine the extent of repair. To study the effect of the MutY variants, MutY deficient cells are first transformed with the appropriate MutY expressing plasmids *(pKK223 MutY).* This is followed by transformation of the substrate containing reporter plasmid.

3.2. Selection of Cloning Vector and Design of Insertion Sequence

The *Ec* strain used for this assay, JM101(mutY:.Tet^R), and the *pkk223.3* expression vector that contains the *Ec muty* gene (eg. *pkkWTMutY)* were kindly provided to us by Dr. M. Michaels and Dr. J. H. Miller (Miller and Michaels, 1996;Michaels, et al., 1990). Variants of

interest are generated via site directed mutagenesis and confirmation of the resultant gene mutation by sequencing. The *pACYC177* reporter plasmid is isolated from ER2424 cells (NEB) using a Promega Miniprep DNA purification system, following the manufacturer's protocol. The plasmid is amplified using *dam*$^-$ GM2929 cells (provided by Dr. M. Marinus (Barras and Marinus, 1989)) to ensure the isolated plasmid is not methylated and does not activate mismatch repair (MMR) proteins that would interfere with MutY-mediated repair (Pukkila, et al., 1983). 10 μg of the isolated plasmid is digested, with 100 units each of *BamHI* and *PstI* (NEB) in the appropriate buffer (NEB 3.1) to generate sticky ends. The double digested plasmid *(pACYC),* purified using a 0.8% agarose gel (prepared in 1X TAE - 40m*M* Tris pH 7.6, 20 m*M* acetic acid and 1 m*M* EDTA pH 8.0) (Table 3) and extracted using Qiagen gel extraction kit, is ligated to 30 pmol of the insert duplex containing OG:A using 15 units of T4 ligase (Promega) followed by purification using a PCR clean-up kit (Qiagen).

The insert duplex, containing the OG:A mispair in a potential *BmtI* recognition site (underlined), has the following sequence:

5' - d(GAT CCG ATC ATG GAG GCT AOGC GCT CCC GTT ACA GCT GCA) - 3' 5' - d(GC TAG TAC CTC CGA T A G CGA GGG CAA TGT CG) - 3'

This duplex is created by individually phosphorylating 300 pmol of each strand with 10 m*M* ATP using T4 PNK (NEB) in the provided buffer. The strands are then combined and annealed in solution with a final duplex concentration of 1 *μM.* A positive control is also prepared by phosphorylating and annealing a duplex with a centrally located G:C base pair in place of the OG:A mispair.

3.3. Electrocompetency and Electroporation Protocol

To ensure maximum transformation efficiency of the plasmids, cells are made freshly electrocompetent. Briefly, a single colony of JM101 from a fresh agar plate is inoculated into 10 ml LB medium dosed with tetracycline (15 mg/ml). The culture is incubated overnight at 37°C and 220 rpm (Table 3). 1.5 ml of this culture, pelleted at 8,000 rpm for 10 mins (Table 3), is used to inoculate 50 ml of 2X YT (3.2 g yeast extract, 2 g tryptone and 1 g NaCl in 200 ml H2O) dosed with tetracycline and allowed to incubate with shaking. When the culture OD_{600nm} reaches 0.6, it is divided equally into three pre-chilled 15 ml centrifuge tubes and cooled in an ice-bath for 30 mins. Meanwhile, all solutions, tubes and pipettes are pre-chilled to 4 °C. The cells are pelleted by centrifugation at 3,000 *g* for 15 min at 4 °C (Table 3), and the supernatant is decanted. The pellet is resuspended sequentially in 14 ml MilliQ H_2O, 10 ml MilliQ H_2O, 4 ml 10% glycerol, and finally in 300 μl of 10% glycerol and pelleted after each resuspension. 50 μl of the final glycerol solution is aliquoted into pre-chilled 0.6 ml microcentrifuge tubes kept ready in an ice tray. The electrocompetent cells hence prepared are best used immediately, but may be stored at −80 °C for up to two weeks.

The MutY expression vector is added to each tube and mixed by pipetting. The cell/DNA mix is then transferred to an electroporation cuvette (Table 3) and pulsed with 1.80 kV (Table 3). SOC medium (300 μl, Invitrogen) is immediately added to the cuvette and used to resuspend and transfer the cells to a 1.6 ml microcentrifuge tube kept on ice. The cells are

then incubated at 37 °C with shaking at 220 rpm for 1 h, following which, 150 μl of each transformation is plated on LB agar plates containing the appropriate antibiotics. Single colonies from this transformation are used to inoculate 10 ml LB dosed with the appropriate antibiotics. The electroporation described above is repeated with the ligated reporter plasmid *(Kan^R),* with one modification: after the hour- long incubation of the cells in SOC medium, equal volumes (150 μl) are used to inoculate agar plates and 10.0 ml LB growth media that are incubated overnight at 37 °C and 220 rpm (Table 3).

3.4. Amplification and Plasmid Extraction

For transformations that produce greater than 100 colonies, the corresponding overnight cultures are used to inoculate 100 ml LB media dosed with the appropriate antibiotics. The cells are allowed to grow until their OD_{600nm} reaches 0.6, after which 100 μl of chloramphenicol is added to each culture and incubation is continued overnight at 37°C and 220 rpm. The cells are then harvested by centrifugation at 10,000 *g* for 10 min at 4 °C (Table 3) and plasmid DNA is isolated using a midiprep kit (Table 3) following the manufacturer's protocol. The concentrations of the recovered plasmids are determined by measuring the A_{260nm} of the samples (Table 3).

3.5. Agarose Gel and Confirmation by Sequencing

To test for MutY-mediate repair of the OG:A base pair in the substrate plasmid to a *Bmtl* site, 1,500 ng of the isolated plasmids are incubated overnight with 20 units of Bmtl-HF (NEB) and its corresponding buffer at 37 °C. The reactions are inhibited by the addition of the provided agarose loading dye, and the fragments are resolved and analyzed by agarose gel electrophoresis using ethidium bromide (2% agarose gel prepared in 1X TAE - 40m*M* Tris pH 7.6, 20 m*M* acetic acid and 1 m*M* EDTA pH 8.0).The bands are visualized by detecting the fluorescence of the DNA intercalator EtBr.

Typically, bands corresponding to both the MutY-expressing plasmid and the reporter plasmid are observed. However, the high percentage of the agarose gel serves to resolve them adequately, and molecular weight bands higher than 3 kb may be disregarded during further analysis. The percent conversion to G:C at the lesion site is determined using the equation (2):

$$\%G{:}C = \frac{I_{1,748} + I_{1,308}}{I_{3,056} + I_{1,748} + I_{1,308}} \text{x} 100 \quad 2$$

In the above equation, I represents the intensity of the indicated molecular weight band. The extent of digestion is assessed by comparing to the digestion of a plasmid carrying a G:C at the lesion site. The percent repair by the each MutY/MUTYH variant is reported as an average of 6 independent transformations ± the standard deviation of these trials. The identity of the base incorporated in the lesion site (G:C or T:A) is confirmed by Sanger sequencing.

3.6. Case Study: Use of bacterial OG:A repair assay to assess relative impacts of catalytic versus binding defects in MutY

Using the bacterial cell assay, we previously evaluated variants of MutY at two key catalytic residues (Asp138, Glu37) and a truncated form of MutY lacking the C-terminal domain (MutY Δ226-350) (Brinkmeyer, et al., 2012). In the S_N1 mechanism for adenine excision catalyzed by MutY, the deprotonated form of Asp138 has been proposed to stabilize the oxacarbenium ion intermediate during the initial adenine departure step as well as mediate formation of a transient covalent acetal intermediate (Woods, et al.,2.16). The protonated form of Glu37 has been proposed to mediate protonation of N7 of adenine to enhance its lability, and then subsequently in its deprotonated state, act as a general base to activate the water molecule in the final hydrolysis step to form the abasic site product (Woods, et al., 2016). The cellular OG:A repair activity of Asp138Glu, Glu37Asp, and Asp138Cys allowed for evaluation of the extent that catalytic defects due to amino acid changes translates into overall repair within a cellular context. Importantly, these three mutated enzymes exhibited similar level of overexpression and stability, allowing differences in repair to be related to rates of adenine excision (k_2) measured *in vitro.* Asp138Glu MutY exhibited similar % G:C at the OG:A lesion as the WT enzyme (100%), consistent with its WT catalytic activity. However, Glu37Asp and Asp138Cys exhibited G:C levels of 68% ± 2% and 47% ± 3% compared to 39% ± 2% G:C in the *muty*⁻ control. The observation of significant levels of OG:A repair mediated by Glu37Asp and Asp138Cys was surprising given that the adenine excision rates were found to be 200 and 600-fold reduced, respectively, compared to the WT enzyme. In contrast, the presence of the C-terminal OG recognition domain (Chmiel, et al., 2001;Wang, et al., 2017) was essential for OG:A- mediated repair in these assays. The percent G:C observed at the OG:A lesion site in cells expressing MutYΔ226-350 was 27% ± 3%, a value similar to that observed in the absence of MutY, despite the fact that the adenine excision rate (k_2) is only reduced 30-fold reduced for MutYΔ226-350 compared to WT MutY. Notably, mutated forms of catalytic residues (e.g. Glu37Asp) retain WT-like high affinity (K_d) for the mismatch as judged by electrophoretic mobility shift assays (EMSA) with an OG:FA substrate analog- containing duplex (Chepanoske, et al., 1999) In contrast, the OG:FA-duplex affinity of MutYΔ226-350 is approximately 200-fold less than WT MutY. These studies illustrated that high affinity for the OG:A substrate is the dominant feature that impacts repair in a cellular context. This is consistent with the arduous task of MutY to identify the OG:A bp within the large excess of undamaged DNA and other DNA-binding proteins in cells.

Troubleshooting tips: Proper ligation of the insert duplex to the double digest plasmid is important for the successful implementation of this assay. We have found that a 1:1 or 1:3 ligation ratio of double digest to insert DNA results in the most successful transformations. However, if fewer than 100 colonies are routinely obtained after electroporation, it may be worthwhile to test different ligation ratios, such as 1:2 or 1:5. Additionally, ligations carried out at 16 °C for 12-14 h have been found to be more efficient than those carried out at room temperature. Another consideration is that the JM101 cell line is *endA*⁺ and therefore the midiprep to recover the plasmids must be done as rapidly as possible to prevent degradation of genomic DNA (which is seen as dark smears near the wells of the agarose gel).

4. A Mammalian Cell Based GFP Reporter Assay

4.1. Evaluating DNA Repair in a Mammalian Cell Based System

The use of purified enzymes and substrates *in vitro* allows for rapid interrogation of amino acid changes that can alter enzyme function. However, cellular assays have the potential to reveal subtle as well as complex protein-substrate and protein-protein interactions. It is somewhat self-evident that studying mammalian enzymes in bacterial cells is not ideal, especially for MUTYH, which has numerous mammalian protein partners (Parker, et al., 2001;Gu, et al., 2002;Hwang, et al., 2015;Turco, et al., 2013;Shi, et al., 2006) and undergoes post-translational modifications not present in bacteria (Kundu, et al., 2010;Dorn, et al., 2014). Following the discovery of MAP in 2002 (Al-Tassan, et al., 2002), further work to study MUTYH variants in mammalian cells hinged on developing MUTYH-deficient mice and their resulting mouse embryonic fibroblast (MEF) cell lines (Hirano, et al., 2003;Russo, et al., 2004;Xie, et al., 2004). The mouse Mutyh enzyme has high sequence homology to the human enzyme, and this was further complimented by utilization of mature gene knockout technology in mice (Lee and Threadgill, 2004). However, methods to determine MUTYH activity in mammalian cells were still under development. For example, Molatore, et al. measured the levels of OG in genomic DNA as a method to evaluate MUTYH-mediated repair (Molatore, et al., 2010); however, it is well-established that MUTYH does not directly remove OG lesions and therefore this assay, at best, is only indirectly reporting on MUTYH activity (McGoldrick, et al., 1995;Pope and David, 2005). A more appropriate assay to directly measure adenine excision in mammalian cells was clearly needed. Here, we detail the approach and methods employed to directly measure OG:A repair in mammalian cells. These methods were used to measure repair in *Mutyh*$^{-/-}$MEFs stably expressing MUTYH variants (Raetz, et al. 2012).

4.2. Design of Mammalian Plasmid Reporter Constructs

The ability to measure the repair of a single lesion type in a quantitative manner in cells necessitates the import of synthetic DNA lesions and ideally a simple way to quantify their repair. A common approach is to introduce a synthetic base lesion into cells within an exogenous reporter construct. There are numerous creative methods developed where a single damaged base placed within a gene region can modulate a reporter gene signal. For example, when placed in the transcribed strand, many DNA lesions block or reduce transcriptional efficiency, which can be quantified as a change in the expression of a measurable gene product such as GFP (green fluorescent protein) (You and Wang, 2015). Others have shown that transcriptional mutagenesis of a strategically placed damaged base results in miscoded RNA products (Doetsch, 2002), which can either activate or inactivate the reporter gene product (Nagel, et al., 2014). Within the context of controlled experiments these signals can be compared against undamaged positive and negative controls to quantify cellular repair.

Here we focus on the measurement of OG:A repair by MUTYH using GFP as a reporter (Raetz, et al., 2012).This general approach can be applied to other lesions, BER glycosylases, and reporter genes. For example, fluorescent and luminescent gene products have been used as reporters in DNA repair assays (Burger, et al., 2010;Masaoka, et al.,

2009). As depicted in Figure 4, this mammalian cell based assay is able to reveal the level of MUTYH mediated repair of OG:A mispairs located within plasmid DNA.

The A to C repair of the GFP gene is amplified by the strong cytomegalovirus (CMV) promoter located upstream of the coding region. Transfection status of individual cells is quantified by the constitutive expression of destabilized red fluorescent protein (dsRed) translated from an internal ribosome entry site (IRES) on the same reporter plasmid (Clonetech). The repair status of individual cells is detected as green fluorescence by flow cytometry. Although endonuclease, polymerase, and ligase activity is required to complete repair on the transcribed strand, this scheme should not require the repair of the OG lesion on the non-template strand. One concern was that cellular pathways that enforce nonsense mediated mRNA destruction would inhibit red fluorescence since the transcript has the stop codon in the GFP cDNA (Lykke-Andersen and Jensen, 2015). However, we found that the same level of red fluorescence was measured both with and without the GFP stop codon, and these constructs were used as GFP-negative and GFP-positive controls in all experiments.

4.3. Production of Plasmid Reporter Constructs

To produce a plasmid DNA construct containing a single site-specific lesion, the first step is to produce a pure closed-circular single-stranded DNA template. The second step is to complete a primer extension reaction that produces a double-stranded DNA that contains the synthetic OG:A mispair. Single-stranded DNA is produced by infecting *Ec* carrying the pGFP-off (GFP^-/$dsRed^+$) plasmid with M13K07 phage and grown overnight at 37 °C and 220 rpm (Table 3). This culture is then centrifuged at 10,000 *g* for 30 minutes (Table 3). The supernatant is combined with 0.2 volumes of precipitation buffer (2.5 *M* NaCl, 20% w/v PEG 8000 (Teknova) and incubated one hour on ice at 4°C. This mixture is centrifuged at 6000 *g* for 30 min at 4 °C (Table 3), and the supernatant decanted. The remaining film formed by the phage is gently resuspended in 10 ml cold TE buffer (10 m*M* Tris pH 7.5, 1 m*M* EDTA pH 8.0) and briefly centrifuged at room temperature, the soluble fraction is decanted and re-precipitated with 0.2 volumes of precipitation buffer, and the pellet is resuspended in cold TE buffer. This process is repeated for a total of three PEG precipitations.

Single-stranded DNA (ssDNA) is extracted from the final phage product by 15 min phenol incubation followed by two phenol/chloroform extractions using Phase Lock gel tubes (5-Prime), and ethanol precipitation. The ssDNA is then resuspended in 10 m*M* Tris pH 7.5 in a volume of 1ml per 200 ml starting culture, typically yielding ssDNA concentrations between 300-800 ng/μl. The amount and purity of the single-stranded DNA is determined by 0.9% agarose gel electrophoresis (Table 3) in TAE buffer.

Second strand synthesis via primer extension begins with phosphorylation and annealing of the OG-containing oligonucleotide to the ssDNA. The oligonucleotide is 5’ phosphorylated using T4 polynucleotide kinase (PNK) per manufactures protocol (NEB), typically with 10 pmol DNA in a total reaction volume of 50 μl. 2-10 μg of single-stranded pIRES2-dsRed-GFP DNA is combined with three-fold molar excess of the phosphorylated oligonucleotide in a final buffer concentration of 28 m*M* Tris-HCl, 5 m*M* $MgCl_2$, 10 m*M* NaCl, and 1 m*M* DTT. To maximize annealing efficiency, the above solution is denatured in 100 °C water,

immediately removed from the heat source and slowly cooled to room temperature. Second strand synthesis and ligation are carried out with the addition of 6% w/v PEG 8,000, 0.6 μg/l bovine serum albumin, 1.5 mM fresh DTT, 1 mM ATP, 0.5 mM dNTPs, 4 units/μl of T4 DNA ligase and 0.5 units/μl of T7 DNA polymerase. This reaction mixture is incubated at 16 °C for 30 min, 37 °C for 1 h, 30 °C for 30 min, 16 °C for 6 h and then held at 4 °C overnight (Table 3). The product must be immediately purified by phenol/chloroform extraction with ethanol precipitation and the product is verified by agarose gel electrophoresis (Table 3) versus single-stranded and double-stranded vector controls.

Importantly, the double-stranded DNA starting material used to produce the singlestranded DNA contains the premature GFP stop codon, thus it cannot be a source of extraneous GFP expression. We have observed that the use of second strand synthesis on a circular single-stranded substrate was hampered by inconsistent yield of the final double-stranded DNA product needed for the assay. The use of nicking enzymes with a double-stranded plasmid substrate with strategically placed restriction sites in the same strand allows for the direct ligation of a short oligonucleotide into a plasmid reporter, and appears to an easier and faster way to produce reporter vectors (You and Wang, 2015).

Troubleshooting tips: The sequence recognized by the nicking enzymes must not be present anywhere else on the plasmid to prevent off target strand scission. In addition, we have found that producing sufficient quantities of the plasmid reporter for mammalian cell culture transfections is the rate-limiting step in performing these cellular repair activity assays. Thus, we highly recommend exploring the use of nicking enzymes and other methods to produce these substrates more efficiently.

4.4. Quantification of Expression with Competitive RT-PCR

To understand how specific amino acid changes in the MUTYH protein alter OG:A DNA repair, we created stable cell lines containing variants using the *Mutyh*$^{-/-}$ MEFs as the parental line. A critical variable was the level of MUTYH expression, since the rate and amount of OG:A repair at any time point is dependent on enzyme expression. Thus, modulating or normalizing for MUTYH expression was a critical aspect of this cell based assay approach. We found that quantification of western blot results was time intensive and not highly consistent and thus turned to measuring MUTYH transcript levels via competitive reverse transcriptase PCR (RT-PCR).

To accurately measure transcription of MUTYH in stably transfected cell lines, competitive RT-PCR is used with a synthetic RNA standard. This standard is created by blunt end ligation of two PCR products, where the products correspond to the 5’ and 3’ ends of the MUTYH transcript. The goal is to create an RNA fragment that will be amplified by the RT-PCR reaction but will have a shorter length. Since this RNA can be carefully quantified before being added to the reaction, it provides a relative reference between band density and the amount of RNA. For MUTYH, a central 337-nucleotide region was removed (MUTYH Δ337), the PCR product inserted into the *pET15b* expression vector (Novagen) and transcribed *in vitro* with T7 RNA polymerase using standard protocols (Green, et al.,

2012;Sambrook, et al., 1989). This RNA standard was quantified by spectrophotometry (Table 3) and stored in small aliquots at −80°C.

For RT-PCR, Trizol-extraction of total RNA from a single well of a six well cell culture plate (approximately 1×10^6 cells) is done based on the manufacturers protocol (Invitrogen). RT-PCR performed using the Qiagen One Step RT-PCR kit using 200 ng of total RNA typically with 1 pg of the MUTYH Δ337 RNA standard per manufacturers protocol. The truncated RNA product is reverse-transcribed and PCR amplified (Table 3) together with any cellular MUTYH mRNA using the same two primers. The resulting PCR reaction will have two products, with the endogenous MUTYH appearing as the full-length product (approximately 800 bp based on our primer locations), whereas the truncated synthetic RNA creates a DNA product of approximately 500 bp. Since both the DNA substrates compete for primers in the same reaction, the relative intensity of these two bands allows for the quantification of MUTYH mRNA to a known quantity of MUTYH RNA. These methods yielded quantification of MUTYH expression that were highly consistent under repeated experiments with the same cell line, allowing for reliable baseline expression level quantification of MUTYH in multiple cell lines.

4.5. Measuring Repair with a GFP Reporter

To measure OG:A repair of the reporter, MEFs are grown to 100% confluency at the time of cell harvest. In our case, we found GFP repair signal was maximized after 3 nights' post-transfection of the reporter plasmid. Typically, 2 μg of plasmid per six well plate is transfected, in parallel with both positive (GFP enabled, no OG insert), and negative (GFP stop codon insert present) conditions. Comparison of GFP signals between cell lines without MUTYH (*Mutyh*$^{-/-}$ MEFs) versus cell lines with normal wild-type MUTYH (WT MEFs) allowed these to be used as comparative baseline measurements of negative and positive controls (respectively) versus cell lines stably transfected with MUTYH variants. MEFs are not known to have high transfection efficiency and transfection reagents can be highly toxic, so careful titration experiments must be performed to determine optimal transfection conditions. Although we typically saw transfection efficiency of only 1% (i.e., 1000 fluorescent events in 100,000 cells processed), the sample of 1,000 events was abundant enough to collect meaningful data. It is typical to be able to process over 100,000 cells for each six-well plate condition.

Cells are harvested for flow cytometry using 0.5% trypsin and washed three times with ice-cold sterile phosphate buffered saline (PBS, pH 7.2), then suspended in ice- cold sterile PBS (pH 7.2) containing 1% paraformaldehyde, and stored at 4°C. Flow cytometry must be completed within 3 h. Events are gated by forward versus side scatter to include only single cells, and the influence in overlap between red and green fluorescence signals is compensated for using a 6-8% compensation level. Three control transfection wells *(pUC18* transfection control, *pGFP-off* (GFP^-/$dsRed^+$), and *pGFP-on* (GFP^+/$dsRed^+$) should be transfected, harvested and analyzed in parallel with the OG:A lesion-containing construct in all experiments.

The data obtained from these experiments can be analyzed using FlowJo Software Version 7.0 (Ashland, OR). We used a simple four-quadrant analysis method to categorize cells with

regard to their red and green fluorescence. With green fluorescence measured on the horizontal scale and red fluorescence on the vertical scale, events (single cells) are categorized as being GFP-positive or GFP-negative. This characterization is based on a vertical quadrant boundary determined by minimizing the number of GFP-negative events in the GFP-positive *(pGFP-on)* transfection, while also symmetrically minimizing the number of GFP-positive events in the GFP-negative *(pGFP-off)* transfection. Additionally, these boundaries are adjusted to maximize exclusion of untransfected cells transfected with a non-fluorescent *pUC18* construct. Non-fluorescent cells are minimized by the position of the horizontal quadrant boundary, while trying to simultaneously maximize legitimate events in the *pGFP-off* (dsRed positive) and *pGFP-on* (dsRed and GFP positive) transfection controls. Lesion repair is calculated as the percent of GFP positive cells in the dsRed (transfection) positive cell population. This calculation is then normalized within each experiment so that the double-positive GFPon/dsRed transfection condition is considered the maximum possible GFP signal. Differences in the ratio of GFP positive cells to GFP negative cells between cell lines is tested for significance using Fisher's exact test with a two-tailed P value. Finally, the standard deviation is calculated from the differences in OG:A repair between multiple experiments.

Troubleshooting tips: OG-containing oligomers are subject to further oxidation or degradation, and thus are best preserved by storing frozen lyophilized aliquots at −80 °C. Both the optimum condition for transfection of plasmid DNA and the harvesting of cells for flow cytometry will greatly depend on the particular cell line under evaluation.

4.6: Case Study: Evaluating MAP variants in mammalian cells

Cancer-associated variants of MUTYH tested with the cellular OG:A repair assay described above led to some key insights. Our results using this assay have shown that the Gly382Asp variant, which was relatively mildly impaired in binding affinity and excision rate (Al-Tassan, et al., 2002), was more significantly impaired in the cellular GFP assay, suggesting that minor differences with *in vitro* assays can be diagnostic for more severe deficiencies in cells. In addition, we showed that even strong overexpression of cancer-associated variant Tyr165Cys at the mRNA level did not compensate for its lack of activity.

Furthermore, we quantified the repair of MEFs stably expressing the common MUTYH polymorphism Gln324His (Raetz, et al., 2012). Although the high allele frequencies of this polymorphism in some ethnic groups suggests that it would be unlikely to significantly alter cellular repair, there is some clinical evidence associating it with higher cancer risk (Kasahara, et al., 2008;Miyaishi, et al., 2009;Picelli, et al., 2010). Indeed, we found the Gln324His variant was significantly less capable of repairing the OG:A reporter plasmid as measured by flow cytometry, evidence of the sensitivity of this assay given the subtle phenotype in humans. Binding and glycosylase assays with purified Gln324His under low salt (60 m*M and* 100 m*M* NaCl) showed adenine excision is similar to WT MUTYH (Brinkmeyer and David, 2015). Interestingly, physiological salt concentrations (150 m*M* NaCl) with Gln324His shows reduced adenine excision (Brinkmeyer and David, 2015), which is similar to the MAP-associated Gly382Asp variant (Raetz, et al., 2012).

5. Summary and Conclusion

Our laboratory has developed and utilized cellular assays to study MutY and MUTYH to better elucidate their roles in facilitating repair of oxidative lesions. The rifampicin resistance assay offers an indirect measurement of DNA repair via the intrinsic mutation rate of *Ec* conferred by antibiotic resistance due to mutations in RNA polymerase. The plasmid-based bacterial repair assay is a more direct measure of repair. It can employ WT MutY, and its variants, as well as synthetic analogs of the natural OG:A substrate, and allows for measurement of the efficiency of cellular lesion search and repair process. Both the rifampicin resistance and bacterial plasmid assays evaluate repair within a bacterial host, which may not possess the same post- translational modifications and protein partners encountered by mammalian homologs. To address this, we have developed a quantitative mammalian cell GFP-based assay that evaluates cellular repair of DNA following transfection of the *MUTYH* gene of interest.

Without the cellular assays, our understanding of MutY enzyme function would be limited to *in vitro* conditions that would not accurately reflect the complexity of the cellular milieu these enzymes function within. For example, *in vitro* assays only minimally replicate the search process of MutY/MUTYH locating DNA damage, and therefore cellular assays more accurately report on these processes by embedding the lesion within a vast excess of undamaged DNA. Taken together, *in vitro* and cellular assays for studying MUTYH provide powerful means to unravel the complex roles played by its unique Fe-S cluster cofactor. Indeed, using such approaches new insights into key molecular features of MutY enzymes, as well as important clinical information on MAP variants has already been revealed, as described in this chapter. Future applications of these approaches for MUTYH and related enzymes will further delineate the complex roles of Fe-S clusters in DNA repair, and the important ways that DNA repair impacts disease.

References

David SS, O'Shea VL, Kundu S, (2007), Base-excision repair of oxidative DNA damage, Nature 447(7147) 941–50. [PubMed: 17581577]

Chepanoske CL, Golinelli MP, Williams SD, David SS, (2000), Positively charged residues within the iron-sulfur cluster loop of E-coli MutY participate in damage recognition and removal, Arch Biochem Biophys 380(1) 11–19. [PubMed: 10900127]

Al-Tassan N, Chmiel NH, Maynard J, Fleming N, Livingston AL, Williams GT, Hodges AK, Davies DR, David SS, Sampson JR, Cheadle JR, (2002), Inherited variants of MYH associated with somatic G : C -> T : A mutations in colorectal tumors, Nat Genet 30(2) 227–232. [PubMed: 11818965]

Jenkins MA, Baglietto L, Dowty JG, Van Vliet CM, Smith L, Mead LJ, Macrae FA, St. John DJB, Jass JR, Giles GG, Hopper JL, Southey MC, (2006), Cancer Risks For Mismatch Repair Gene Mutation Carriers: A Population-Based Early Onset Case-Family Study, Clinical Gastroenterology and Hepatology 4(4) 489–498. [PubMed: 16616355]

Farrington SM, Tenesa A, Barnetson R, Wiltshire A, Prendergast J, Porteous M, Campbell H, Dunlop MG, (2005), Germline susceptibility to colorectal cancer due to base- excision repair gene defects, American journal of human genetics 77(1) 112–9. [PubMed: 15931596]

Sieber OM, Lipton L, Crabtree M, Heinimann K, Fidalgo P, Phillips RK, Bisgaard ML, Orntoft TF, Aaltonen LA, Hodgson SV, Thomas HJ, Tomlinson IP, (2003), Multiple colorectal adenomas,

classic adenomatous polyposis, and germ-line mutations in MYH, The New England journal of medicine 348(9) 791–9. [PubMed: 12606733]

Viel A, Bruselles A, Meccia E, Fornasarig M, Quaia M, Canzonieri V, Policicchio E, Urso ED, Agostini M, Genuardi M, Lucci-Cordisco E, Venesio T, Martayan A, Diodoro MG, Sanchez-Mete L, Stigliano V, Mazzei F, Grasso F, Giuliani A, Baiocchi M, Maestro R, Giannini G, Tartaglia M, Alexandrov LB, Bignami M, (2017), A Specific Mutational Signature Associated with DNA 8-Oxoguanine Persistence in MUTYH-defective Colorectal Cancer, EBioMedicine 20 39–49. [PubMed: 28551381]

Banda DM, Nuñez NN, Burnside MA, Bradshaw KM, David SS, (2017), Repair of 8- oxoG:A mismatches by the MUTYH glycosylase: Mechanism, metals and medicine, Free Radical Biology and Medicine 107 202–215. [PubMed: 28087410]

Chmiel NH, Livingston AL, David SS, (2003), Insight into the functional consequences of inherited variants of the hMYH adenine glycosylase associated with colorectal cancer: complementation assays with hMYH variants and pre-steady-state kinetics of the corresponding mutated E.coli enzymes, J Mol Biol 327(2) 431–43. [PubMed: 12628248]

Engstrom LM, Brinkmeyer MK, Ha Y, Raetz AG, Hedman B, Hodgson KO, Solomon EI, David SS, (2014), A zinc linchpin motif in the MUTYH glycosylase interdomain connector is required for efficient repair of DNA damage, J Am Chem Soc 136(22) 7829–32. [PubMed: 24841533]

Pope MA, David SS, (2005), DNA damage recognition and repair by the murine MutY homologue, DNA Repair 4(1) 91–102. [PubMed: 15533841]

Brinkmeyer MK, David SS, (2015), Distinct functional consequences of MUTYH variants associated with colorectal cancer: Damaged DNA affinity, glycosylase activity and interaction with PCNA and Husl, DNA Repair (Amst) 34 39–51. [PubMed: 26377631]

Kundu S, Brinkmeyer MK, Livingston AL, David SS, (2009), Adenine removal activity and bacterial complementation with the human MutY homologue (MUTYH) and Y165C, G382D, P391L and Q324R variants associated with colorectal cancer, DNA Repair (Amst) 8(12) 1400–10. [PubMed: 19836313]

David SS, O'Shea VL, Kundu S, (2007), Base-excision repair of oxidative DNA damage, Nature 447(7147) 941–950. [PubMed: 17581577]

Fry RC, Svensson JP, Valiathan C, Wang E, Hogan BJ, Bhattacharya S, Bugni JM, Whittaker CA, Samson LD, (2008), Genomic predictors of interindividual differences in response to DNA damaging agents, Genes & development 22(19) 2621–6. [PubMed: 18805990]

Kundu S, Brinkmeyer MK, Eigenheer RA, David SS, (2010), Ser 524 is a phosphorylation site in MUTYH and Ser 524 mutations alter 8-oxoguanine (OG): A mismatch recognition, DNA Repair 9(10) 1026–1037. [PubMed: 20724227]

Dorn J, Ferrari E, Imhof R, Ziegler N, Hubscher U, (2014), Regulation of human MutYH DNA glycosylase by the E3 ubiquitin ligase mule, J Biol Chem 289(10) 7049–58. [PubMed: 24443563]

Amouroux R, Campalans A, Epe B, Radicella JP, (2010), Oxidative stress triggers the preferential assembly of base excision repair complexes on open chromatin regions, Nucleic Acids Res 38(9) 2878–2890. [PubMed: 20071746]

Menoni H, Di Mascio P, Cadet J, Dimitrov S, Angelov D, (2017), Chromatin associated mechanisms in base excision repair - nucleosome remodeling and DNA transcription, two key players, Free Radic Biol Med 107 159–169. [PubMed: 28011149]

Parker A, Gu Y, Mahoney W, Lee SH, Singh KK, Lu AL, (2001), Human homolog of the MutY repair protein (hMYH) physically interacts with proteins involved in long patch DNA base excision repair, J Biol Chem 276(8) 5547–55. [PubMed: 11092888]

Gu Y, Parker A, Wilson TM, Bai H, Chang DY, Lu AL, (2002), Human MutY homolog, a DNA glycosylase involved in base excision repair, physically and functionally interacts with mismatch repair proteins human MutS homolog 2/human MutS homolog 6, J Biol Chem 277(13) 11135–42. [PubMed: 11801590]

Hwang BJ, Jin J, Gao Y, Shi G, Madabushi A, Yan A, Guan X, Zalzman M, Nakajima S, Lan L, Lu AL, (2015), SIRT6 protein deacetylase interacts with MYH DNA glycosylase, APE1 endonuclease, and Rad9-Rad1-Hus1 checkpoint clamp, BMC molecular biology 16 12. [PubMed: 26063178]

Turco E, Ventura I, Minoprio A, Russo MT, Torreri P, Degan P, Molatore S, Ranzani GN, Bignami M, Mazzei F, (2013), Understanding the role of the Q338H MUTYH variant in oxidative damage repair, Nucleic Acids Res 41(7) 4093–103. [PubMed: 23460202]

Shi G, Chang DY, Cheng CC, Guan X, Venclovas C, Lu AL, (2006), Physical and functional interactions between MutY glycosylase homologue (MYH) and checkpoint proteins Rad9- Rad1-Hus1, The Biochemical journal 400(1) 53–62. [PubMed: 16879101]

Manlove AH, Nuñez NN, David SS, 2016 The GO Repair Pathway: OGG1 and MUTYH, The Base Excision Repair Pathway, WORLD SCIENTIFIC pp. 63–115.

Manlove AH, McKibbin PL, Doyle EL, Majumdar C, Hamm ML, David SS, (2017), Structure-Activity Relationships Reveal Key Features of 8-Oxoguanine: A Mismatch Detection by the MutY Glycosylase, ACS Chemical Biology.

Livingston AL, O'Shea VL, Kim T, Kool ET, David SS, (2008), Unnatural substrates reveal the importance of 8-oxoguanine for in vivo mismatch repair by MutY, Nat Chem Biol 4(1) 51–58. [PubMed: 18026095]

Brinkmeyer MK, Pope MA, David SS, (2012), Catalytic Contributions of Key Residues in the Adenine Glycosylase MutY Revealed by pH-dependent Kinetics and Cellular Repair Assays, Chem Biol 19(2) 276–286. [PubMed: 22365610]

Chepanoske CL, Porello SL, Fujiwara T, Sugiyama H, David SS, (1999), Substrate recognition by Escherichia coli MutY using substrate analogs, Nucleic Acids Res 27(15) 3197–3204. [PubMed: 10454618]

Golinelli MP, Chmiel NH, David SS, (1999), Site-directed mutagenesis of the cysteine ligands to the [4Fe4S] cluster of Escherichia coli MutY, BiochemistryUs 38(22) 6997–7007.

Raetz AG, Xie Y, Kundu S, Brinkmeyer MK, Chang C, David SS, (2012), Cancer-associated variants and a common polymorphism of MUTYH exhibit reduced repair of oxidative DNA damage using a GFP-based assay in mammalian cells, Carcinogenesis 33(11) 2301–9. [PubMed: 22926731]

Miller JH, Michaels M, (1996), Finding new mutator strains of Escherichia coli--a review, Gene 179(1) 129–32. [PubMed: 8955638]

David SS, Wiliams SD, (1998), Chemistry of glycosylases and endonucleases involved in base-excision repair, Chem Rev 98(3) 1221–1261. [PubMed: 11848931]

Wehrli W, Knüsel F, Schmid K, Staehelin M, (1968), Interaction of rifamycin with bacterial RNA polymerase, Proceedings of the National Academy of Sciences 61(2) 667–673.

Garibyan L, Huang T, Kim M, Wolff E, Nguyen A, Nguyen T, Diep A, Hu K, Iverson A, Yang H, Miller JH, (2003), Use of the rpoB gene to determine the specificity of base substitution mutations on the Escherichia coli chromosome, DNA Repair (Amst) 2(5) 593–608. [PubMed: 12713816]

Slupska MM, Luther WM, Chiang JH, Yang H, Miller JH, (1999), Functional expression of hMYH, a human homolog of the Escherichia coli MutY protein, J Bacteriol 181(19) 6210–3. [PubMed: 10498741]

Michaels ML, Cruz C, Grollman AP, Miller JH, (1992), Evidence that MutY and MutM combine to prevent mutations by an oxidatively damaged form of guanine in DNA, Proceedings of the National Academy of Sciences 89(15) 7022–7025.

Lodish H, Berk A, Zipursky SL, Matsudaira P, Baltimore D, Darnell J, (2000), Molecular cell biology 4th edition, National Center for Biotechnology InformationÕs Bookshelf.

Foster PL, (2006), Methods for determining spontaneous mutation rates, Methods Enzymol 409 195–213. [PubMed: 16793403]

Rosche WA, Foster PL, (2000), Determining mutation rates in bacterial populations, Methods 20(1) 4–17. [PubMed: 10610800]

Zheng Q, (2015), A new practical guide to the Luria-Delbrück protocol, Mutation Research/Fundamental and Molecular Mechanisms of Mutagenesis 781 7–13. [PubMed: 26366669]

Sarkar S, Ma WT, Sandri GH, (1992), On fluctuation analysis: a new, simple and efficient method for computing the expected number of mutants, Genetica 85(2) 173–9. [PubMed: 1624139]

Couce A, Blazquez J, (2011), Estimating mutation rates in low-replication experiments, Mutat Res 714(1–2) 26–32. [PubMed: 21736881]

Gillet-Markowska A, Louvel G, Fischer G, (2015), bz-rates: A Web Tool to Estimate Mutation Rates from Fluctuation Analysis, G3: Genes|Genomes|Genetics 5(11) 2323–2327. [PubMed: 26338660]

Wolff E, Kim M, Hu K, Yang H, Miller JH, (2004), Polymerases Leave Fingerprints: Analysis of the Mutational Spectrum in Escherichia coli rpoB To Assess the Role of Polymerase IV in Spontaneous Mutation, Journal of Bacteriology 186(9) 2900–2905. [PubMed: 15090533]

Chmiel NH, Livingston AL, David SS, (2003), Insight into the functional consequences of inherited variants of the hMYH adenine glycosylase associated with colorectal cancer: Complementation assays with hMYH variants, and pre-steady-state kinetics of the corresponding mutated E-coli enzymes, J Mol Biol 327(2) 431–443. [PubMed: 12628248]

Porello SL, Leyes AE, David SS, (1998), Single-turnover and pre-steady-state kinetics of the reaction of the adenine glycosylase MutY with mismatch-containing DNA substrates, Biochemistry-Us 37(42) 14756–14764.

Livingston AL, O'Shea VL, Kim T, Kool ET, David SS, (2008), Unnatural substrates reveal the importance of 8-oxoguanine for in vivo mismatch repair by MutY, Nat Chem Biol 4(1) 51–58. [PubMed: 18026095]

Michaels ML, Pham L, Nghiem Y, Cruz C, Miller JH, (1990), MutY, an adenine glycosylase active on G-A mispairs, has homology to endonuclease III, Nucleic Acids Res 18(13) 3841–5. [PubMed: 2197596]

Barras F, Marinus MG, (1989), The great GATC: DNA methylation in E. coli, Trends in Genetics 5 139–143. [PubMed: 2667217]

Pukkila PJ, Peterson J, Herman G, Modrich P, Meselson M, (1983), EFFECTS OF HIGH LEVELS OF DNA ADENINE METHYLATION ON METHYL-DIRECTED MISMATCH REPAIR IN ESCHERICHIA COLI, Genetics 104(4) 571–582. [PubMed: 6225697]

Woods RD, O'Shea VL, Chu A, Cao S, Richards JL, Horvath MP, David SS, (2016), Structure and stereochemistry of the base excision repair glycosylase MutY reveal a mechanism similar to retaining glycosidases, Nucleic Acids Res 44(2) 801–810. [PubMed: 26673696]

Chmiel NH, Golinelli MP, Francis AW, David SS, (2001), Efficient recognition of substrates and substrate analogs by the adenine glycosylase MutY requires the C-terminal domain, Nucleic Acids Res 29(2) 553–564. [PubMed: 11139626]

Wang L, Chakravarthy S, Verdine GL, (2017), Structural Basis for the Lesion-scanning Mechanism of the MutY DNA Glycosylase, J Biol Chem 292(12) 5007–5017. [PubMed: 28130451]

Hirano S, Tominaga Y, Ichinoe A, Ushijima Y, Tsuchimoto D, Honda-Ohnishi Y, Ohtsubo T, Sakumi K, Nakabeppu Y, (2003), Mutator phenotype of MUTYH-null mouse embryonic stem cells, J Biol Chem 278(40) 38121–4. [PubMed: 12917422]

Russo MT, De Luca G, Degan P, Parlanti E, Dogliotti E, Barnes DE, Lindahl T, Yang H, Miller JH, Bignami M, (2004), Accumulation of the oxidative base lesion 8-hydroxyguanine in DNA of tumor-prone mice defective in both the Myh and Ogg1 DNA glycosylases, Cancer research 64(13) 4411–4. [PubMed: 15231648]

Xie Y, Yang H, Cunanan C, Okamoto K, Shibata D, Pan J, Barnes DE, Lindahl T, McIlhatton M, Fishel R, Miller JH, (2004), Deficiencies in mouse Myh and Ogg1 result in tumor predisposition and G to T mutations in codon 12 of the K-ras oncogene in lung tumors, Cancer research 64(9) 3096–102. [PubMed: 15126346]

Lee D, Threadgill DW, (2004), Investigating gene function using mouse models, Current opinion in genetics & development 14(3) 246–252. [PubMed: 15172666]

Molatore S, Russo MT, D'Agostino VG, Barone F, Matsumoto Y, Albertini AM, Minoprio A, Degan P, Mazzei F, Bignami M, Ranzani GN, (2010), MUTYH mutations associated with familial adenomatous polyposis: functional characterization by a mammalian cell-based assay, Human mutation 31(2) 159–66. [PubMed: 19953527]

McGoldrick JP, Yeh YC, Solomon M, Essigmann JM, Lu AL, (1995), Characterization of a mammalian homolog of the Escherichia coli MutY mismatch repair protein, Molecular and cellular biology 15(2) 989–96. [PubMed: 7823963]

Pope MA, David SS, (2005), DNA damage recognition and repair by the murine MutY homologue, DNA repair 4(1) 91–102. [PubMed: 15533841]

You C, Wang Y, (2015), Quantitative measurement of transcriptional inhibition and mutagenesis induced by site-specifically incorporated DNA lesions in vitro and in vivo, Nature protocols 10(9) 1389–406. [PubMed: 26292071]

Doetsch PW, (2002), Translesion synthesis by RNA polymerases: occurrence and biological implications for transcriptional mutagenesis, Mutat Res 510(1–2) 131–40. [PubMed: 12459449]

Nagel ZD, Margulies CM, Chaim IA, McRee SK, Mazzucato P, Ahmad A, Abo RP, Butty VL, Forget AL, Samson LD, (2014), Multiplexed DNA repair assays for multiple lesions and multiple doses via transcription inhibition and transcriptional mutagenesis, Proc Natl Acad Sci U S A 111(18) E1823–32. [PubMed: 24757057]

Raetz AG, Xie YL, Kundu S, Brinkmeyer MK, Chang C, David SS, (2012), Cancer- associated variants and a common polymorphism of MUTYH exhibit reduced repair of oxidative DNA damage using a GFP-based assay in mammalian cells, Carcinogenesis 33(11) 2301–2309. [PubMed: 22926731]

Burger K, Matt K, Kieser N, Gebhard D, Bergemann J, (2010), A modified fluorimetric host cell reactivation assay to determine the repair capacity of primary keratinocytes, melanocytes and fibroblasts, BMC Biotechnol 10 46. [PubMed: 20569452]

Masaoka A, Horton JK, Beard WA, Wilson SH, (2009), DNA polymerase beta and PARP activities in base excision repair in living cells, DNA Repair (Amst) 8(11) 1290–9. [PubMed: 19748837]

Lykke-Andersen S, Jensen TH, (2015), Nonsense-mediated mRNA decay: an intricate machinery that shapes transcriptomes, Nature reviews. Molecular cell biology 16(11) 665–77. [PubMed: 26397022]

Green MR, Sambrook J, Sambrook J, 2012Molecular cloning : a laboratory manual, 4th ed., Cold Spring Harbor Laboratory Press, Cold Spring Harbor, N.Y.

Sambrook J, Fritsch EF, Maniatis T, 1989Molecular cloning: a laboratory manual, Cold Spring Harbor Laboratory Press, Cold Spring Harbor, NY.

Al-Tassan N, Chmiel NH, Maynard J, Fleming N, Livingston AL, Williams GT, Hodges AK, Davies DR, David SS, Sampson JR, Cheadle JP, (2002), Inherited variants of MYH associated with somatic G:C-->T:A mutations in colorectal tumors, Nature genetics 30(2) 227–32. [PubMed: 11818965]

Raetz AG, Xie Y, Kundu S, Brinkmeyer MK, Chang C, David SS, (2012), Cancer-associated variants and a common polymorphism of MUTYH exhibit reduced repair of oxidative DNA damage using a GFP-based assay in mammalian cells, Carcinogenesis.

Kasahara M, Osawa K, Yoshida K, Miyaishi A, Osawa Y, Inoue N, Tsutou A, Tabuchi Y, Tanaka K, Yamamoto M, Shimada E, Takahashi J, (2008), Association of MUTYH Gln324His and APEX1 Asp148Glu with colorectal cancer and smoking in a Japanese population, Journal of experimental & clinical cancer research : CR 27 49. [PubMed: 18823566]

Miyaishi A, Osawa K, Osawa Y, Inoue N, Yoshida K, Kasahara M, Tsutou A, Tabuchi Y, Sakamoto K, Tsubota N, Takahashi J, (2009), MUTYH Gln324His gene polymorphism and genetic susceptibility for lung cancer in a Japanese population, Journal of experimental & clinical cancer research : CR 28 10. [PubMed: 19161591]

Picelli S, Zajac P, Zhou XL, Edler D, Lenander C, Dalen J, Hjern F, Lundqvist N, Lindforss U, Pahlman L, Smedh K, Tornqvist A, Holm J, Janson M, Andersson M, Ekelund S, Olsson L, Lundeberg J, Lindblom A, (2010), Common variants in human CRC genes as low- risk alleles, Eur J Cancer 46(6) 1041–8. [PubMed: 20149637]

Luncsford PJ, Chang DY, Shi G, Bernstein J, Madabushi A, Patterson DN, Lu AL, Toth EA, (2010), A structural hinge in eukaryotic MutY homologues mediates catalytic activity and Rad9-Rad1-Hus1 checkpoint complex interactions, J Mol Biol 403(3) 351–70. [PubMed: 20816984]

Out AA, Tops CM, Nielsen M, Weiss MM, van Minderhout IJ, Fokkema IF, Buisine MP, Claes K, Colas C, Fodde R, Fostira F, Franken PF, Gaustadnes M, Heinimann K, Hodgson SV, Hogervorst FB, Holinski-Feder E, Lagerstedt-Robinson K, Olschwang S, van den Ouweland AM, Redeker EJ, Scott RJ, Vankeirsbilck B, Gronlund RV, Wijnen JT, Wikman FP, Aretz S, Sampson JR, Devilee P, den Dunnen JT, Hes FJ, (2010), Leiden Open Variation Database of the MUTYH gene, Human mutation 31(11) 1205–15. [PubMed: 20725929]

Tsien RY, (1998), The green fluorescent protein, Annual review of biochemistry 67 509–44.

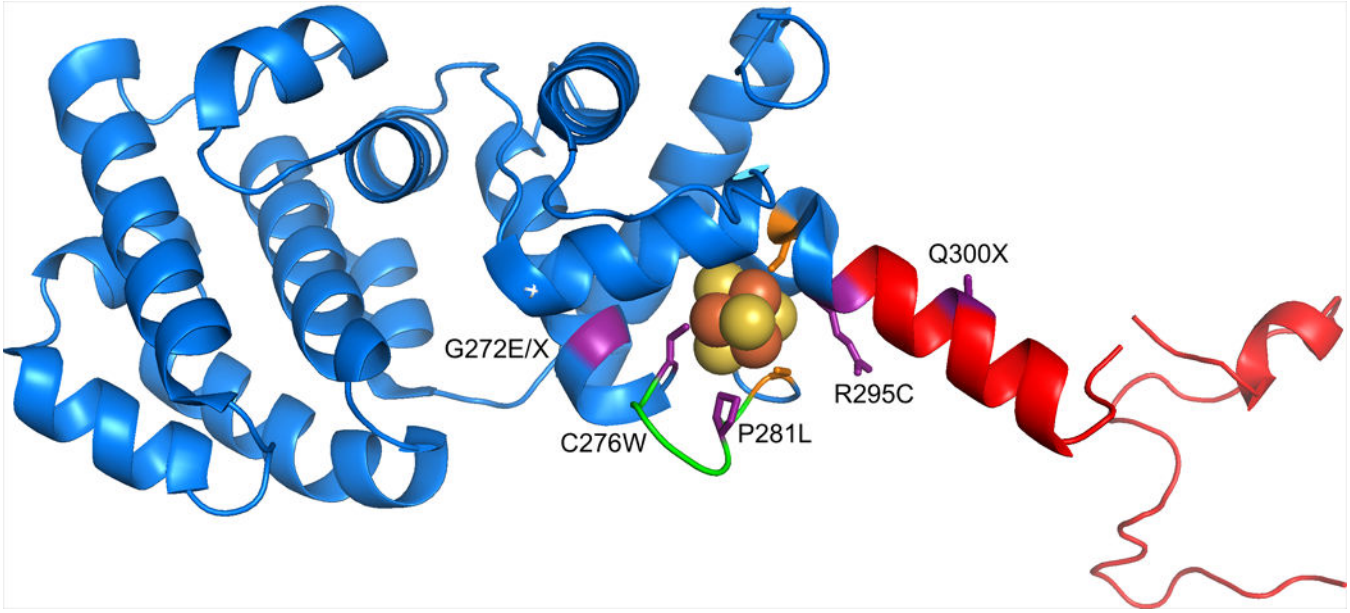

Figure 1: Fe-S cluster in MUTYH.

N-terminal fragment crystal structure of *Homo sapiens* (Hs) MUTYH (PDB 3N5N) depicting the position of MAP variants adjacent the Fe-S cluster (Luncsford, et al., 2010). The N-terminal domain is in blue, the FCL in green, IDC in red, the Fe-S cluster coordinating Cys ligands in orange, and reported MAP variants in purple, where X denotes a nonsense mutation (Out, et al., 2010).

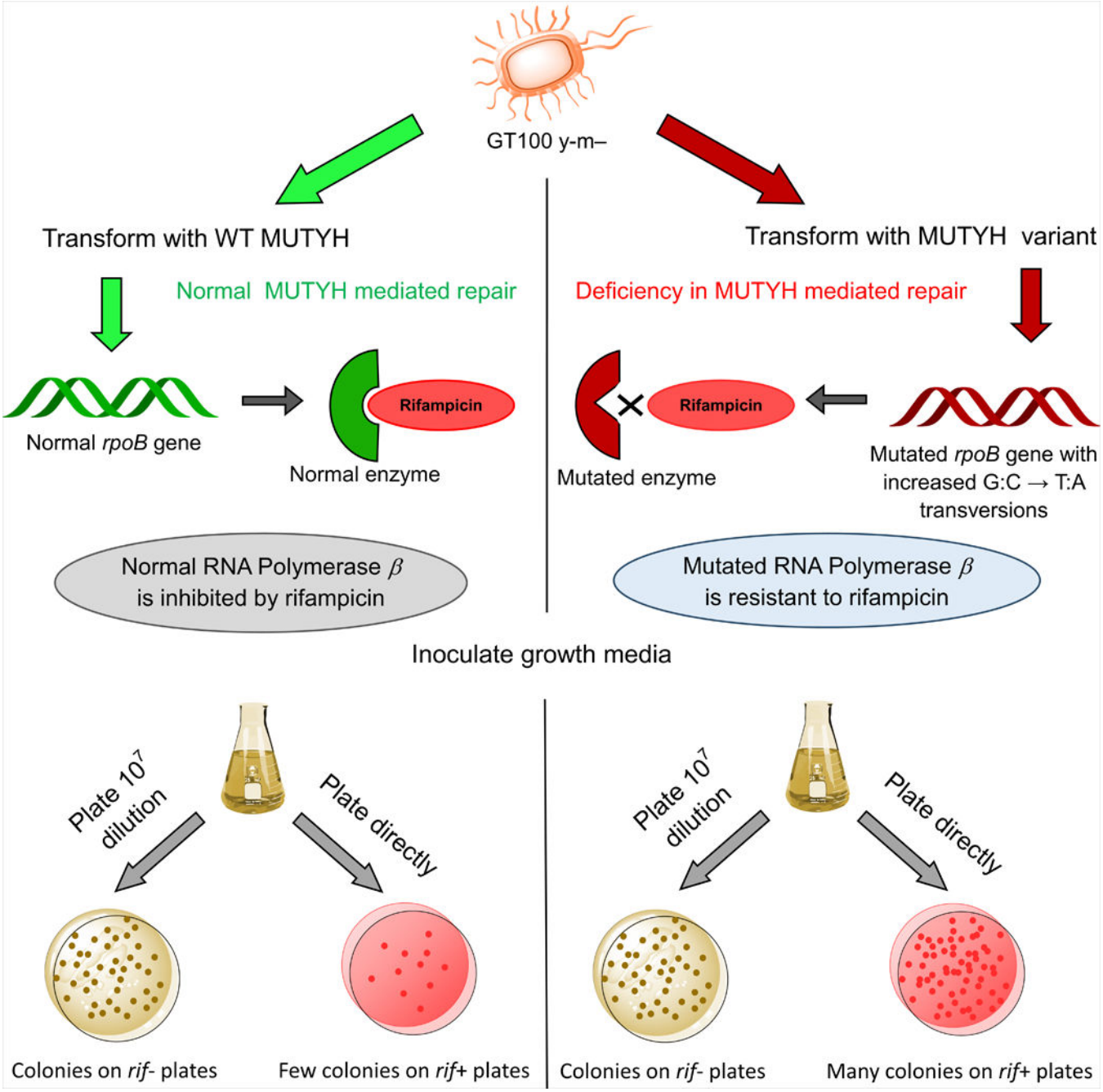

Figure 2: Schematic representation of the rifampicin resistance assay.

This assay is used to establish the cellular mutation frequency and correlate these mutagenesis events to deficiencies in MUTYH mediated repair. This assay is accomplished through counting the number of colonies resistant to rifampicin (depicted as red plates) in comparison to samples grown on a non-rifampicin containing plate (depicted in brown). The ratio of the median number of resistant colonies to the average number of viable colonies from the corresponding cultures is used to determine the mutation frequency (Garibyan, et al., 2003).

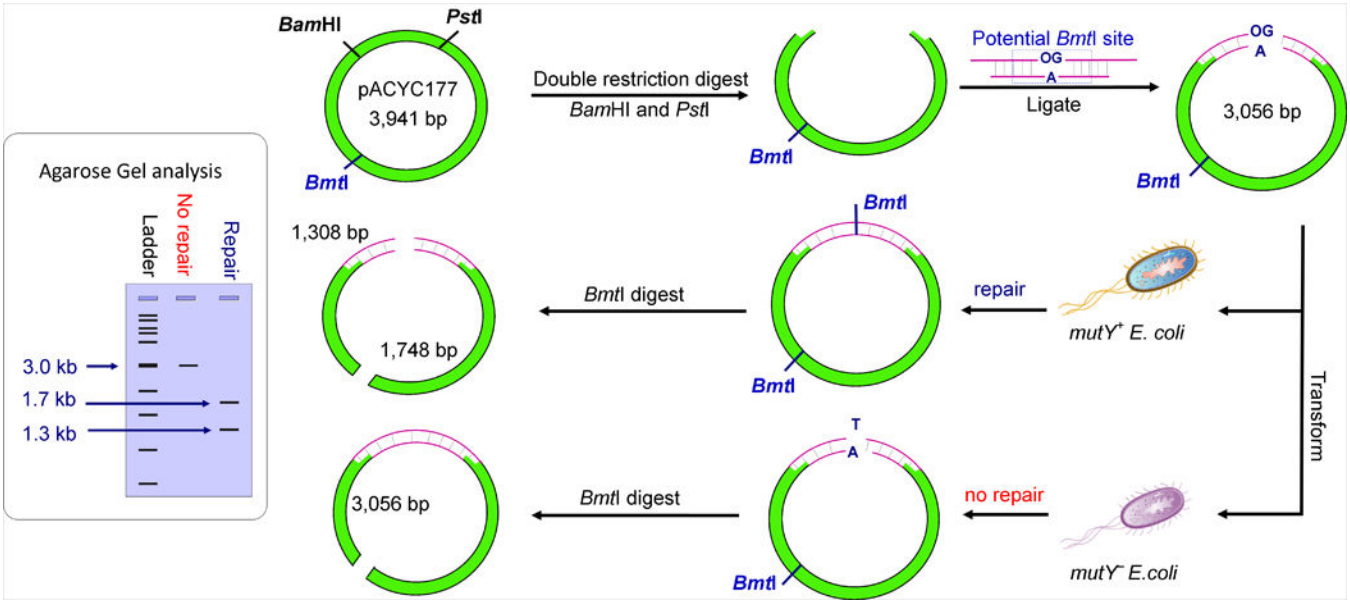

Figure 3: Schematic representation of the plasmid based bacterial cell assay to assay MutY-mediated OG:A repair.

The restriction enzyme sites for *BamHI, PstI* and *BmtI* are indicated on the *pACYC177* (green) plasmid, and the insert duplex carrying the OG:A mispair is shown in pink. The representative agarose gel on the left shows the expected bands formed after *BmtI* digestion of the recovered plasmids. To analyze MutY variants, *muty⁻ Ec* are transformed with the appropriate vector expressing the mutant enzyme and compared to the results from cells transformed with plasmids expressing the WT enzyme (Brinkmeyer, et al., 2012).

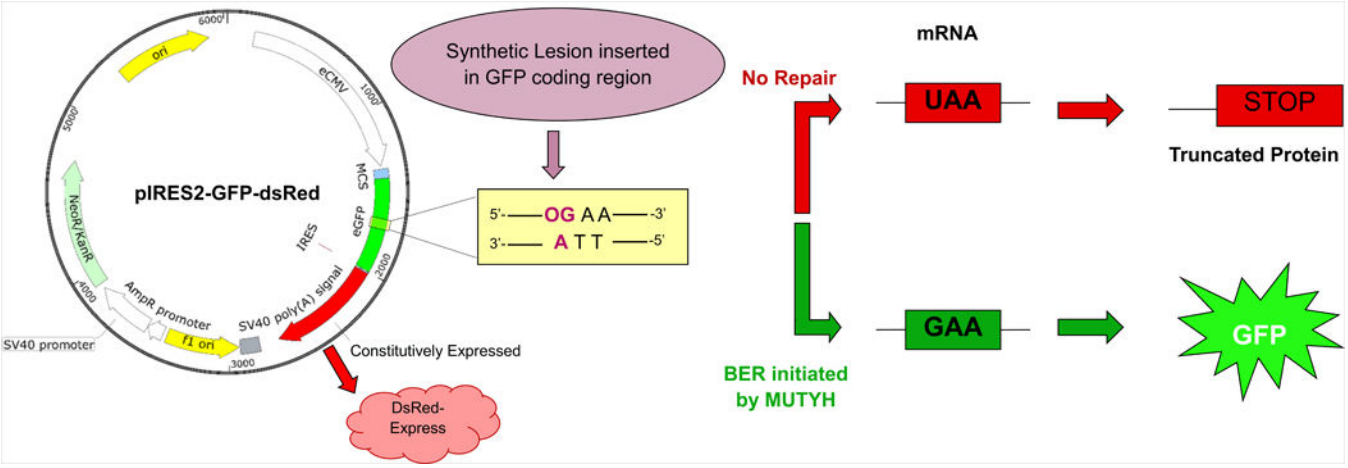

Figure 4: Schematic representation of the GFP reporter assay. Repair of the OG:A base pair initiated by MUTYH results in GFP expression.

Here, a chemically synthesized OG containing nucleotide is placed opposite A within the coding region of the GFP reporter construct. By default, full GFP expression is interrupted with a stop codon, leading to a 33 amino acid truncated protein product that does not contain the chromophore core needed for fluorescence (Tsien, 1998). However, excision of A and subsequent repair to C causes the complementary mRNA codon to change from UAA to GAA, and translation of this change restores the wild-type amino acid, Glu, allowing expression of full-length wild-type green fluorescent protein.

Table 1

Agar and Media Composition for the Rifampicin Resistance Assay

Culture Agar	Culture Media	Rifampicin Agar
LB media	LB media	LB media
15 μg/ml tetracycline	15 μg/ml tetracycline	15 μg/ml tetracycline
100 μg/ml ampicillin	100 μg/ml ampicillin	100 μg/ml ampicillin
50 m*M* agar		100 μg/mL rifampicin
		50 m*M* agar

Table 2

Rifampicin resistance assay example data for calculating mutation rate per cell division, corresponding to the median number of colonies for number of mutants (rifampicin resistant) or average number of total cells (viable).

	Wild-type MUTYH		Cys325Ser MUTYH	
Culture number	**Number of Mutants**	**Total Cells (10^7)**	**Number of Mutants**	**Total Cells (10^7)**
1	14	562	114	462
2	38	478	158	842
3	16	493	120	637
4	26	526	121	615
5	6	483	105	350
6	25	501	133	450
7	104	633	182	500
8	24	373	127	850
9	12	540	136	510
10	6	370	162	648
11	50	650	104	350
12	21	471	142	596
13	10	672	203	806
14	6	406	307	850
15	34	487	131	528
16	N/A	N/A	106	674
Trial totals	21	510	132	604
Mutation rate per cell division	6×10^{-10}		5×10^{-9}	
95% confidence interval	$4 \times 10^{-10} - 8 \times 10^{-10}$		$3 \times 10^{-9} - 6 \times 10^{-9}$	

Table 3

Summary of equipment needed for MutY/MUTYH cell based assays

Equipment	Notable Specifications
Pipette tips/microcentrifuge tubes/conical tubes	DNase/RNase/Pyrogen free and sterile
Vortex/mini centrifuge	Table top
Thermocycler	Applied Biosystems GeneAmp PCR System 2400
Incubator/shaker	Temperature/speed control
Stir/hot plate	Temperature control
Centrifuge	Sorvall Ultracentrifuge
Sonifier	Branson sonifier 250 at 70% power
UV/vis	HP 8453 with OLISWorks
Electroporator and cuvettes	Bio-Rad MicroPulser Electroporator and Bio-Rad gene pulser cuvettes, 0.1 cm
Midiprep kit	Promega Wizard midiprep kit
Western blot/SDS gel equipment	Bio-Rad
Agarose gel equipment	Bio-rad mini sub gel gt
Flow Cytometer	Becton Dickinson FACScan Flow cytometer
Cold room	Maintained at 4 °C